Understanding Light- and Elevated Temperature-Induced Degradation in Silicon Wafers Using Hydrogen Effusion Mass Spectroscopy

Sahar Jafari, Utkarshaa Varshney, Bram Hoex, Sylke Meyer, and Dominik Lausch

***Abstract*—Hydrogen has been long known for its ability to passivate defects in silicon devices. However, multiple recent studies on understanding the mechanism behind light- and elevated temperature-induced degradation (LeTID) have proposed that hydrogen plays an important role in this degradation mechanism. Despite its important role in photovoltaic applications, the quantitative assessment of hydrogen is difficult and seldom reported. In this work, we applied hydrogen effusion mass spectroscopy to quantify the hydrogen released from hydrogenated silicon nitride (SiN_x:H) and atomic layer deposited (ALD) aluminum oxide (AlO_x) dielectric films at elevated temperatures. We demonstrate that the amount of hydrogen effused from these layers strongly correlates with the extent of LeTID observed in the multicrystalline silicon wafers passivated with these monolayers and their stacks. It is shown that the hydrogen effusion scales linearly with the SiN_x:H thickness, similar as the extent of LeTID. The effusion measurements on the AlO_x/SiN_x:H stack revealed that the presence of the AlO_x film modifies the total amount of hydrogen that is effused, whereas it was found to slow the hydrogen in-diffusion. This result is consistent with the LeTID extent determined after contact firing where ALD AlO_x layers were found to act as a hydrogen diffusion barrier, strongly reducing LeTID when placed in between c-Si and SiN_x:H and increasing LeTID when placed on top of SiN_x:H.**

***Index Terms*—Diffusion, effusion measurement, hydrogen, light- and elevated temperature-induced degradation (LeTID), surface passivation.**

I. Introduction

HYDROGENATED amorphous layers have been known to provide a high level of surface passivation that assists in achieving highly efficient silicon solar cells. Dielectric layers, such as amorphous silicon nitride (a-SiN_x:H) and amorphous silicon (a-Si_x:H), typically grown by plasma-enhanced chemical vapor deposition (PECVD) have, therefore, been investigated over the past forty years [1]–[3]. In addition to providing excellent passivation, it is well known that these layers release hydrogen during the contact firing step, which is essential for metallization and is typically done at temperatures of $\sim$ 800–900 °C. These temperatures are high enough to release a significant amount of hydrogen from the hydrogenated PECVD films and most of the hydrogen effuses into the air. A fraction of this hydrogen diffuses into the silicon bulk and passivates the crystallographic defects and accelerates the recovery of the carrier-induced defects, such as the boron–oxygen defect [4]–[7]. However, recently there is a growing body of the literature that indicates the involvement of this bulk hydrogen in causing light- and elevated temperature-induced degradation (LeTID) [8]–[11]. This degradation phenomenon has been the focus of multiple research groups worldwide as it causes significant degradation in all silicon wafer types [9], [12]–[14] and is particularly prominent in the industry standard passivated emitter rear contact cells [15], [16]. Although the root cause of LeTID is hitherto unknown, multiple studies that showed its relationship pertaining to numerous physical and processing parameters have surfaced crucial empirical trends correlating them with the rate and extent of degradation. Its extent has been reported to increase with the firing temperature [18]–[20], overall thermal budget [10], [21]–[23], and variation in surface passivation [24]–[28]. All these relationships have pointed toward a strong correlation of LeTID with bulk hydrogen concentration [11].

The diagnosis and tracking of hydrogen (being the lightest element) requires highly sensitive measuring systems. Therefore, most publications that speculate about the involvement of hydrogen in LeTID only reported qualitative characterization. However, some studies have reported a relationship between LeTID and hydrogen released from SiN_x:H using Fourier-transform infrared spectroscopy (FTIR) [25], [29]. A recent publication from Walter *et al.* [30] reported a direct method to measure the hydrogen concentration in float-zone silicon (FZ-Si) by measuring the change in resistivity after hydrogen bonds to form boron–hydrogen pairs. However, this technique is not suitable in the case of multicrystalline silicon (mc-Si) wafers as the bulk material consists of multiple (in addition to boron) hydrogen sinks (such as grain boundaries and dislocations [31]), however, using it with parallelly processed FZ-Si samples

Manuscript received January 7, 2021; revised February 28, 2021, June 10, 2021, and July 12, 2021; accepted August 3, 2021. Date of publication September 9, 2021; date of current version October 21, 2021. This work was supported in part by the Fraunhofer Center for Silicon Photovoltaics CSP within the joint research project NexTec-Wafer 333003 and in part by Australian Government through the Australian Renewable Energy Agency under Grant 2017/RND010, Grant 2017/RND007, and Grant 1-A060. *(Corresponding authors: Sahar Jafari; Utkarshaa Varshney.)*

Sahar Jafari and Sylke Meyer are with the Fraunhofer Center for Silicon Photovoltaics CSP, 06120 Halle, Germany (e-mail: saharjafari86@gmail.com; sylke.meyer@csp.fraunhofer.de).

Utkarshaa Varshney and Bram Hoex are with the School of Photovoltaic and Renewable Energy Engineering, University of New South Wales, Sydney, NSW 2052, Australia (e-mail: u.varshney@unsw.edu.au; b.hoex@unsw.edu.au).

Dominik Lausch is with Denkweit GmbH, 06108 Halle, Germany (e-mail: dominik.lausch@denkweit.de).

Color versions of one or more figures in this article are available at https://doi.org/10.1109/JPHOTOV.2021.3104194.

Digital Object Identifier 10.1109/JPHOTOV.2021.3104194

provides a feasible approach [11]. Some frequently used characterization methods are FTIR [32], secondary ion mass spectroscopy (SIMS) [33], elastic recoil detection analysis (ERDA) [34], and nuclear reaction analysis (NRA) [35]. However, NRA, ERDA, and SIMS are costly, time consuming, and not readily available. FTIR spectroscopy is one of the common methods, but it only detects hydrogen bonded to other elements. Hydrogen effusion mass spectroscopy is an alternative method for measuring the molecular hydrogen that is released from a heated sample [36], and its application in examining the cause of LeTID is presented in this study.

Beyer [37] established and developed the hydrogen effusion mass spectroscopy for studying the role of hydrogen in hydrogenated silicon films in the saturation of dangling bonds at the surface and interface with the main focus on a-Si_x:H films. The study of glow-discharge a-SiN_x:H alloys via effusion measurements performed in 1987 showed that the addition of nitrogen atoms to amorphous hydrogenated silicon material shifts the hydrogen effusion peak to a higher temperature, which was correlated with the higher binding energy of nitrogen–hydrogen bonds (N–H) [38]. Later in 1996, Murley *et al.* [39] applied both FTIR spectroscopy and hydrogen effusion measurements to analyze the role of deposition parameters on the film composition of SiN_x:H. In 2006, Beyer and Dekkers [40] reported the application of effusion measurements for studying the microstructure of a-SiN_x:H films and showed that the effusion of hydrogen from a porous network is in the form of hydrogen molecules while in compact material, atomic hydrogen is the dominant diffusing species. Recently, we have developed a simplified setup for effusion measurements to focus more on the hydrogen-related mechanisms in photovoltaic (PV) applications. We reported that hydrogen effusion is limited by the film composition, and a N-gradient SiN_x:H stacked layer reduced the hydrogen effusion at annealing temperatures, which could not be observed from FTIR measurements [41].

This work aims to improve the physical understanding of the LeTID mechanism and the underlying role of hydrogen. We have applied hydrogen effusion measurements for the first time to study the LeTID phenomenon in silicon wafers coated with various hydrogenated thin films. The authors are aware that fast firing is vastly different from the relatively slower annealing performed in effusion measurements, however, this analysis hitherto provides some valuable insights in understanding the degradation phenomenon. The results showed that the hydrogen evolution from the SiN_x:H layers correlates with the layer thickness and aligns well with normalized defect density (NDD) when the samples were tested for LeTID. Furthermore, we study aluminum oxide/silicon nitride (AlO_x:/SiN_x:H) passivation stacks and observed an early release of hydrogen from AlO_x film in the form of double peaks at 400–500 °C in contrast with the relatively N-rich SiN_x:H, which peaks at ∼900 °C. Overall, the effusion measurements strongly support the hypothesis of the involvement of hydrogen in LeTID in our samples.

II. Experiment

A. Sample Preparation and Characterization

Commercial isotextured 156 × 156 mm boron-doped p-type Czochralski-Si (Cz-Si) wafers of resistivity ∼1 Ω·cm and thickness ∼180 μm and mc-Si (sister) wafers of resistivity ∼1.6 Ω·cm and thickness ∼180 μm were selected. The wafers were cleaned using the standard Radio Corporation of America 1 and 2 processes, followed by a short hydrofluoric acid (HF) dip to remove any oxides from the surfaces. All the wafers then underwent a gettering $POCl_3$ diffusion, which resulted in heavy n^+ regions. These layers were chemically etched back by a solution of HF and nitric acid (HNO_3). The samples were then passivated to make two sets of minority carrier lifetime test structures.

1) *For the first set*, SiN_x:H layers (of refractive index ∼2.02 at 630 nm) of different thicknesses were deposited on both sides of the wafer using remote PECVD (Roth and Rau MAiA) at 400 °C to create symmetrical lifetime structures. To vary the thickness of SiN_x:H, the belt speed in the tool was doubled (104 cm/min) to obtain the thinnest layer (SiN_x-1–50 nm). Subsequent depositions were done using the same recipe by repeating the process two, three, and four times, respectively, to achieve variable SiN_x:H thicknesses (SiN_x-2–100 nm, SiN_x-3–150 nm, and SiN_x-4–200 nm). The mc-Si samples were then fired at a set peak temperature of 855 °C (actual sample temperature of 770 ± 3 °C) at a constant belt speed of 450 cm/min in an industrial belt furnace (Schmid Sierra Therm) to test for LeTID. The Cz-Si wafers did not undergo the firing step and were directly used for the effusion measurements. The actual thermal profiles were measured on identical wafers using a Q18 Datapaq thermal profiler. Precise details can be found in an earlier publication [26].
2) *For the second set,* the samples were passivated with the following:
   a) PECVD-based SiN_x:H with a thickness ∼80 nm and refractive index ∼ 2.02;
   b) SiN_x:H capped with atomic layer deposited (ALD) AlO_x with a thickness ∼7 nm deposited at 250 °C [Si/SiN_x:H/AlO_x];
   c) AlO_x capped with SiN_x:H [Si/AlO_x/SiN_x:H].

The details of the process can be found in [27]. The samples were then fired at a set peak temperature of 830 °C. The Cz-Si samples did not undergo firing and were only used for the effusion measurements.

B. LeTID Testing

The mc-Si samples underwent accelerated LeTID testing using a 938-nm high-intensity laser illumination of 26.6 and 38 kW/m^2 [42] at 130 °C for set one and two, respectively. It is worth noting that the difference in the illumination intensities occurred due to an upgrade in our laser system.

The progression in effective minority carrier lifetime $\tau_{\rm eff}$ was measured using a photoconductance decay lifetime tester from Sinton instruments (WCT-120TS) at room temperature. For comparison between degradation extents, NDD was calculated [43] as

$$\mathrm{NDD} = \frac{1}{\tau(\mathrm{t})} - \frac{1}{\tau_{\rm fired}} \tag{1}$$

where $\tau(\mathrm{t})$ and $\tau_{\rm fired}$ are the effective lifetimes at time *t* during testing and right after firing, respectively. In every case, the effective lifetime values were extracted at an injection level (Δn) equal to 0.1 times the base doping density.

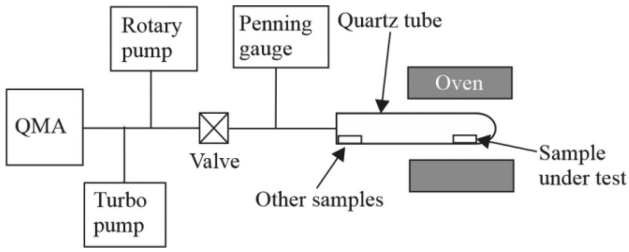

Fig. 1. Schematic of effusion mass spectroscopy system.

C. Hydrogen Effusion Measurement

For the hydrogen effusion measurements, the as-deposited Cz-Si samples were laser cut in a size of 5 × 5 mm before inserting them into the effusion mass spectroscopy setup. A schematic of the setup can be found in Fig. 1 [41], [44].

A quartz tube with a length of 25 cm and an outer diameter of 16 mm was used as a vacuum chamber in this system, which was sealed from one side and constantly pumped out from the other side. The samples were mounted on small nickel boats that were adjusted under vacuum from the outside of the quartz tube via a small magnet. The oven was mounted on a railway and could move toward the quartz tube. To measure a sample, it was placed in the end part of the tube (right side) where it was heated in the oven. The rest of the samples were kept in the cold part of the tube (left side) away from the heated range. Before the test sample was transferred, this heated part of the quartz tube was baked at 1000 °C for 10 min to remove any residual hydrogen.

Before every measurement, a reference measurement was carried out to determine the background H_2 concentration in the measurement setup and this value was subtracted from the sample measurements. The samples were heated from room temperature to 1000 °C at a constant heating rate (β) of 20 °C/min and the partial H_2 pressure in the chamber was measured as a function of the annealing temperature.

III. Results

A. Influence of SiN_x:H Thickness

The FTIR absorption spectra of the samples with different SiN_x:H thicknesses before and after firing were reported earlier in [26]. With a particular focus on the hydrogen-related bonds, the results indicated a trend of increasing absorbance for both [Si–H] and [N–H] bonds with the increase in SiN_x:H thickness, which indicates an increase in hydrogen content with the film thickness.

The mc-Si samples passivated with different thicknesses of SiN_x:H were tested for LeTID at 130 °C under 26.6 kW/m^2 illumination intensity. The progression of NDD has been reported previously in [26] and shown in Fig. 2. The extent of maximum degradation is about seven times for SiN_x-4 as compared with SiN_x-1. Inset shows that for our experimental range, the increase in degradation is approximately linear with the SiN_x:H thickness.

Moreover, the partial pressure of effused hydrogen gas molecules from this set of samples (nonfired Cz-Si samples) is displayed in Fig. 3 as a function of annealing temperature. The results clearly show that there is an increase in hydrogen effusion

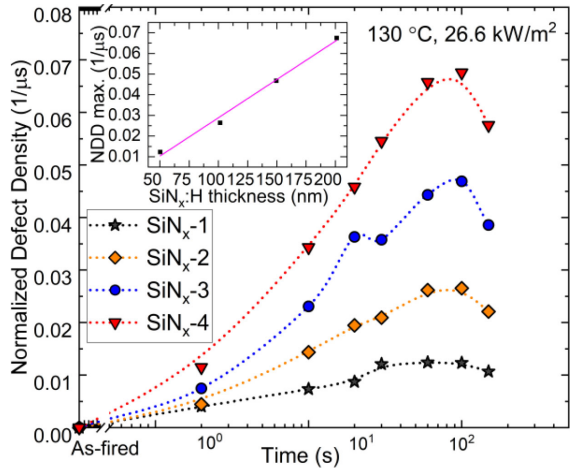

Fig. 2. Evolution of NDD versus cumulative laser time when the mc-Si samples passivated with multiple SiN_x:H thicknesses were tested under accelerated degradation conditions of 26.6 kW/m^2 at 130 °C. The connected lines are guide to the eye. The data in the inset show the trend of maximum degradation with SiN_x:H thickness. The data have been adapted from the article presented in [26].

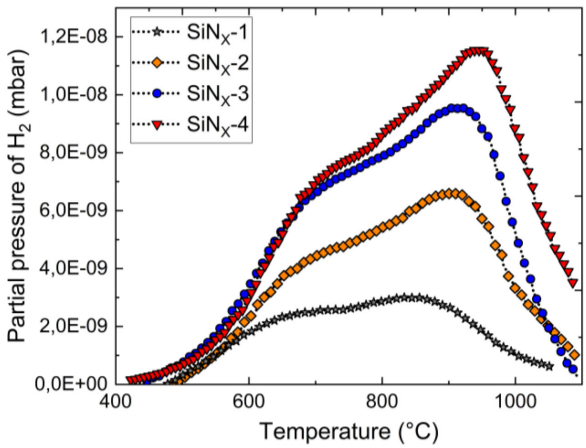

Fig. 3. Hydrogen effusion spectra of set 1 sample passivated with SiN_x:H films of various thicknesses.

with the increase in film thickness. The hydrogen spectra of SiN_x:H show the typical two-component peak structure for all the samples, one at low temperature (LT) of about 700 °C and a second peak at high temperature (HT) of ∼900 °C. It is worth noting that the second peak shifts from 850 °C in SiN_x-1 (thickness of ∼50 nm) to 950 °C in SiN_x-4 (thickness of ∼200 nm). This difference can be attributed to the increase of the hydrogen diffusion coefficient, which is proportional to the film thickness [45].

B. Influence of AlO_x

The strong impact of adding thin ALD AlO_x films in the passivation stack on the extent of LeTID in mc-Si wafers has been reported earlier in [27]. Fig. 4 highlights the influence of surface layers on the intensity of maximum degradation. It shows that the Si/SiN_x:H/AlO_x (AlO_x as a capping layer for SiN_x:H) sample showed maximum LeTID. In contrast, lowest NDD_{max} was observed for Si/AlO_x/SiN_x:H wafer.

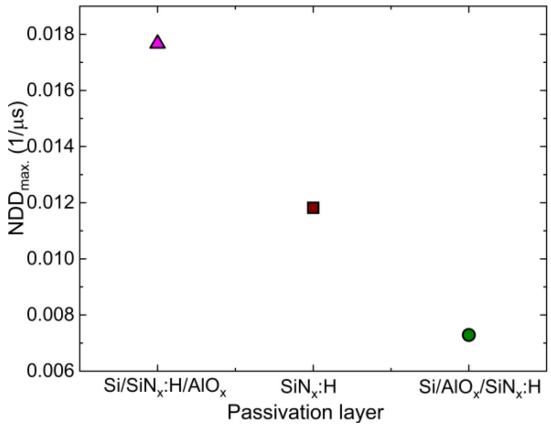

Fig. 4. NDD_{max} for the samples passivated with variable SiN_x:H and AlO_x based stacks when tested for LeTID under the illumination intensity of 38 kW/m^2 at 130 °C. The data are adapted from the article presented in [27].

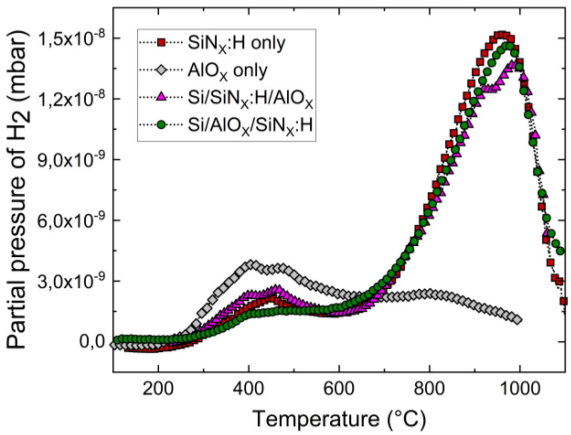

Fig. 5. Partial pressure of molecular hydrogen H_2 effused from the sample set 2.

In addition to the LeTID test, the hydrogen effusion spectra of the second set of samples were measured and shown in Fig. 5. The partial pressure of the hydrogen effusion from two monolayers of SiN_x:H and AlO_x as well as the stacked layers of Si/AlO_x/SiN_x:H and Si/SiN_x:H/AlO_x are plotted as a function of annealing temperature. A relatively low hydrogen release was observed from the single AlO_x film. The maximum effusion occurs at a temperature of ∼400 °C [46], where the peak has a double peak structure. The effusion spectrum of the SiN_x:H film consisted of a small peak at an LT (LT peak) of ∼450 °C, followed by a large peak at an HT (HT peak) of ∼950 °C as explained earlier in [38]. It was reported that the amount of hydrogen-related bonds in PECVD grown SiN_x:H was ∼eight times higher than that of ALD AlO_x layer [27]. However, based on the integral of the hydrogen effusion measurement, the amount of total hydrogen effused from the SiN_x:H layer was only a factor of ∼3 compared with ALD AlO_x layers and this will be discussed later in this article. Nevertheless, ALD AlO_x contains significant lower hydrogen-related bonds than SiN_x:H and are well known to be comparatively hydrogen lean.

The hydrogen effusion from the Si/SiN_x/AlO_x and Si/AlO_x/SiN_x samples was very similar to the Si/SiN_x sample with a clear LT and HT peak. However, for the Si/SiN_x/AlO_x sample, a double peak was visible around 400 °C, which is very similar to the Si/AlO_x sample. The HT peak for the Si/SiN_x/AlO_x also has its maximum at a higher temperature compared with the other samples, this will be discussed in more detail in Section IV.

IV. Discussion

The aforementioned results indicated a correlation between hydrogen effusion from different hydrogenated layers (and their stacks) during annealing at a constant heating rate and the extent of LeTID after firing. The knowledge of the film composition and the associated hydrogen mobility from the effusion measurements can expand our understanding of the hydrogen diffusion mechanism at elevated temperatures and its involvement in LeTID. This section details the comparison of HT firing with slow annealing during effusion experiments and the potential role of hydrogen in LeTID.

A. Comparison of Effusion Experiments With the HT Firing

Since the time scale of the firing and effusion experiments varies significantly, a series of effusion measurements were carried out in a preheated oven near the typical firing temperature. For this purpose, five SiN_x:H films (Samples A–E) were deposited on FZ-Si wafers by PECVD technique using different gas flow ratios of NH_3/SiH_4 to achieve films with different compositions. Subsequently, these samples were all measured at a constant oven temperature of 700 °C for 5 min.

The results for Samples A and B, as shown in Fig. 6(a), show that the normalized partial pressure of hydrogen P_{H_2} had a maximum in the first few seconds, followed by an exponential drop. The exponential decay was fitted by

$$P_{H_2} = P_0\, e^{-Rt}. \tag{2}$$

The decay constant *R* reduces with the reduction of effused hydrogen in different samples. As our system has a constant pumping rate, it can be derived that the change in H_2 concentration N_{H_2} over time is [36]

$$\frac{\partial N_{H_2}}{\partial t} \propto P_{H_2} \tag{3}$$

which means that the total amount of effused hydrogen can easily be obtained by integrating (2) to $t = \infty$. The total amount of effused hydrogen when using a constant heating rate can be calculated using

$$\int_{T_0}^{T\max} P_{H_2} dT]_{\beta}. \tag{4}$$

Table I lists the integral values for five different SiN_x:H layers. The temperature integral of the partial pressure is calculated up to 700 °C for the effusion spectra, while the area under the exponential fit was incremented until it drops to zero.

The results show a linear correlation between the two measurements. This implies that the effusion of hydrogen from SiN_x:H is strongly temperature dependent and the main part of diffusion/effusion occurs at a given temperature within the first few seconds. Therefore, the effusion measurement with a constant heating rate would also provide a comparable measure of the effused hydrogen during a rapid annealing process.

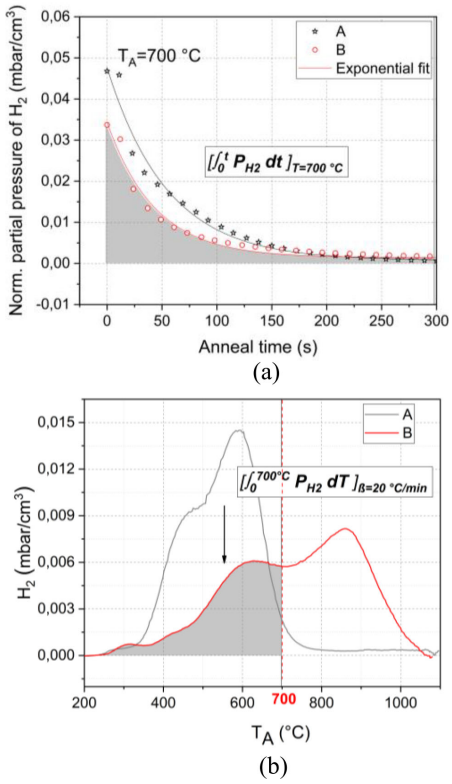

Fig. 6. (a) Partial pressure of effused hydrogen decreased exponentially when the samples were exposed to a constant temperature of 700 °C for a few minutes. (b) Hydrogen effusion spectra of two SiN_x:H films, A and B, at constant heating rate of ß=20 °C/min. The time integral of normalized partial pressure of effused hydrogen P_{H_2} at constant temperature is proportional to the temperature integral of normalized P_{H_2} at constant heating rate, shown by gray areas under exponential fit and the effusion spectrum.

TABLE I
TIME INTEGRAL OF NORMALIZED PARTIAL PRESSURE OF EFFUSED HYDROGEN P_{H_2} AT CONSTANT TEMPERATURE $T = T_{\text{firing}}$ IS PROPORTIONAL TO THE TEMPERATURE INTEGRAL OF P_{H_2} AT CONSTANT HEATING RATE

Sample	$[\int_o^{t_{total}} P_{H_2} dt]_{T=700\,^\circ C}$ (a.u.)	$[\int_{T_0}^{T=700\,^\circ C} P_{H_2} dT]_\beta$ (a.u.)
A	2.86	2.75
B	2.64	2.65
C	2.55	2.32
D	2.11	1.86
E	1.97	1.82

B. Influence of Hydrogen Concentration on LeTID

The effusion measurements revealed that more hydrogen effused from thicker SiN_x:H layers during annealing (see Fig. 3). Fig. 7 illustrates the maximum values of NDD in the first set of samples obtained in Fig. 2 versus integrated area under the effusion spectra up to an annealing temperature of 850 °C. The actual sample temperature during the effusion measurement was not measured and only the oven temperature was considered. Therefore, the peak temperature during firing was chosen for the comparison. Van Wieringen and Warmoltz [47] and Sheoran *et al.* [48] showed that the hydrogenation in crystalline silicon (c-Si) at HT is not diffusion limited. Consequently, it is reasonable to assume that the effusion in the ambient and in-diffusion of

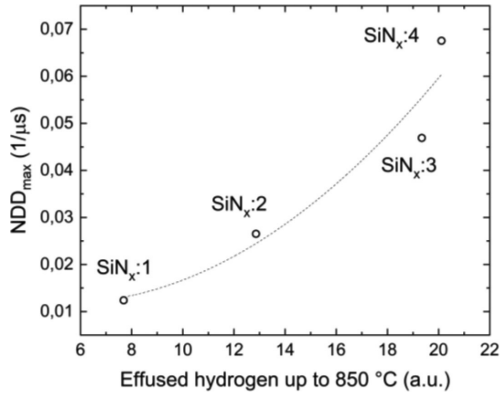

Fig. 7. Maximum normalized defect densities ($NDD_{\max}$) of the samples passivated with multiple thicknesses of SiN_x:H layers versus integrated area under the effusion spectra up to temperature of ~850 °C. The line is a guide to the eyes.

hydrogen in bulk are correlated. Thus, more hydrogen effusion indicates that potentially more hydrogen would be diffused into the substrate, leading to a higher NDD. It suggests that more hydrogen being present at the interfaces and in the bulk could assist in the formation of the LeTID defect within the bulk material during light soaking. Hence, the presented trend between NDD and the effused H-content is consistent with a hydrogen-related defect responsible for the observed degradation. However, the difference between maximum NDD measured in SiN_x-1 and SiN_x-4 was about seven times, whereas the amount of effused hydrogen from SiN_x-4 is only three times higher than SiN_x-1.The shape of the effusion spectra in Fig. 3 did not change significantly due to the increase in film thickness. This means that the composition of SiN_x:H is independent of the deposition time and, therefore, its thickness. It is known that during effusion measurements [38], the hydrogen released from SiN_x:H films at LT is attributed to the H_2 molecules desorbing from the surface, followed by hydrogen atoms from the rupturing of the Si–H bonds below 800 °C. A linear increase in the hydrogen effusion with the increase in film thickness was observed with an exception of SiN_x-3. In contrast, the peak at HT is ascribed to the hydrogen from the bonds with higher binding energy, such as N–H. In Fig. 3, the HT peak of hydrogen shifts to the higher annealing temperatures by increasing the layer thickness. This was earlier reported by Beyer and Wagner [45] and explained by the fact that the effusion measurement is affected by the diffusion of hydrogen through the SiN_x:H film. The diffusion-limited effusion of hydrogen could, thus, have resulted in a shift of the HT peak toward higher temperatures for thicker SiN_x:H films at a constant heating rate.

On the other hand, the extent of the LeTID increased significantly with SiN_x:H thickness. However, the increase in NDD and effused hydrogen is not linearly correlated. This is possibly the result of inaccuracy of sampling and measurements, and another unknown defect candidate playing a role in LeTID. The latter is highly likely as a possibility of metallic impurities affecting the LeTID extent that has been reported earlier [11], [19], [49], [50].

The combination of two methods, FTIR [26] and effusion mass spectroscopy also revealed some information about the film composition and the mechanism of hydrogen transport in

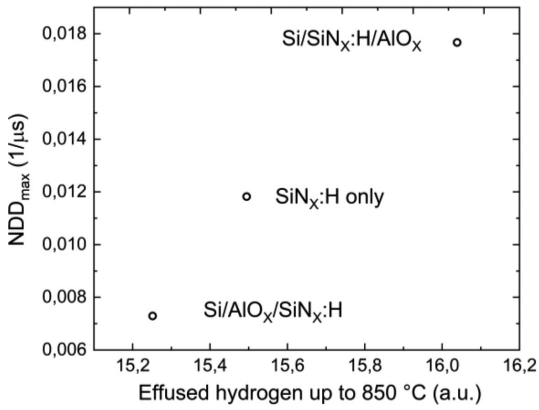

Fig. 8. NDD_{max} of sample passivated with variable SiN_x:H and AlO_x stacks as a function of integrated area under the effusion spectra up to temperature of ∼850 °C.

SiN_x:H. FTIR showed that the N–H bonds are the primary hydrogen bonds in the films, which explains the reasoning behind the HT peak being the maxima in the effusion spectra. Moreover, from FTIR, we also observed that the N–H related IR peak reduced after firing, which explains the release of hydrogen from SiN_x:H films during HT firing. However, Si–H related IR peak increased, which has also been reported earlier by Verlaan *et al.* [51], and has been explained by the increase in the density of the films after annealing, which changes the proportionality constant, which may result in an increase in FTIR peak while the bond concentration actually decreased.

Considering effusion spectra of these films with LT peak below 800 °C, it can be assumed that almost all the Si–H bonds would be broken during firing. The increase in Si–H bonds after firing can then be described by the freed hydrogen diffusion in the film, meeting silicon dangling bonds and forming new Si–H bonds. However, the position of the HT peak is at ∼850 °C, thus the typical firing temperature is not sufficient to break all N–H bonds and the freed hydrogen is more likely to bond with silicon atoms than nitrogen. In this regard, we have previously reported that the increase of N content in SiN_x:H film can work as a barrier to hydrogen getting diffused [41].

C. AlO_x as a Barrier for Hydrogen Effusion

In the second set of samples, the influence of AlO_x layers on the evolution of NDD and the hydrogen effusion mechanism has been studied.

The double peak structure in hydrogen effusion spectra of a single AlO_x film at LT would potentially be attributed to loss of hydrogen in two forms, −OH bonds and molecular hydrogen (H_2) present in the AlO_x:H film or at its surface [52]. The stacked layer of Si/SiN_x:H/AlO_x is the closest to AlO_x:H monolayer since the AlO_x is the topmost layer in both the cases. This would mean that the hydrogen effusion from the Si/SiN_x:H/AlO_x at LT is attributed to AlO_x layer and at higher temperature to SiN_x:H.

In Fig. 8, we show the NDD_{max} as a function of the effused hydrogen up to 850 °C. It can be seen that there is only a very small difference between the total amount of hydrogen effused from all three samples, while a significant difference in NDD_{max} was measured. This could most likely be attributed to the significantly lower hydrogen diffusion coefficient in ALD AlO_x, which inhibits hydrogen effusion to the ambient when it is the top film or hydrogen diffusion to the Si bulk when it is in between Si and SiN_x:H during a rapid firing step while the impact is relatively minimal during a slow thermal effusion experiment.

V. Conclusion

In this work, we investigated the role of hydrogen in LeTID by measuring the hydrogen effusion from the samples during HT firing and comparing it with the defect density introduced via accelerated LeTID testing. We tested the samples passivated with different SiN_x:H thicknesses and a direct correlation among the increase in SiN_x:H thickness, effused hydrogen content, and the LeTID extent was found. It affirms the speculations of the significant role of hydrogen in the generation of defects that lead to bulk degradation pertaining to LeTID. However, the increase in NDD and hydrogen effusion was not linearly correlated.

In addition, minor changes in the total hydrogen effusion were observed when AlO_x layers were used. A single AlO_x layer has a relatively higher hydrogen effusion at LTs (and much lower than SiN_x:H passivated samples) below 500 °C, likely resulting from surface H_2 and H_2O. The total amount of hydrogen effused from thin film stacks of AlO_x and SiN_x:H was found to be very similar, while significant differences in LeTID were detected. The hydrogen effusion measurements indicated a slower hydrogen diffusion when AlO_x was used as the top layer, which is consistent with the hypothesis that ALD AlO_x layers act as a hydrogen barrier during a rapid thermal anneal. However, the understanding of the AlO_x as a barrier to hydrogen effusion requires further work.

Acknowledgment

The authors would like to thank Prof. W. Beyer at Jülich Research Center for his kind support and knowledgeable advices.

References

[1] T. Lauinger, J. Moschner, A. G. Aberle, and R. Hezel, "Optimization and characterization of remote plasma-enhanced chemical vapor deposition silicon nitride for the passivation of p-type crystalline silicon surfaces," *J. Vac. Sci. Technol. A*, vol. 16, no. 2, pp. 530–543, 1998, doi: 10.1116/1.581095.

[2] H. MäcKel and R. Lüdemann, "Detailed study of the composition of hydrogenated SiNx layers for high-quality silicon surface passivation," *J. Appl. Phys.*, vol. 92, no. 5, pp. 2602–2609, 2002, doi: 10.1063/1.1495529.

[3] R. Hezel and R. Schörner, "Plasma Si nitride—A promising dielectric to achieve high-quality silicon MIS/IL solar cells," *J. Appl. Phys.*, vol. 52, no. 4, pp. 3076–3079, 1981, doi: 10.1063/1.329058.

[4] S. Wilking, A. Herguth, and G. Hahn, "Influence of hydrogenated passivation layers on the regeneration of boron-oxygen related defects," *Energy Procedia*, vol. 38, pp. 642–648, 2013, doi: 10.1016/j.egypro.2013.07.328.

[5] N. Nampalli, B. Hallam, C. Chan, M. Abbott, and S. Wenham, "Role of hydrogen in the permanent passivation of boron-oxygen defects in czochralski silicon," in *Proc. IEEE 42nd Photovolt. Specialist Conf.*, 2015, pp. 1–3, doi: 10.1109/PVSC.2015.7356404.

[6] B. J. Hallam *et al.*, "Advanced hydrogenation of dislocation clusters and boron-oxygen defects in silicon solar cells," *Energy Procedia*, vol. 77, pp. 799–809, 2015, doi: 10.1016/j.egypro.2015.07.113.

[7] M. Gläser and D. Lausch, "Towards a quantitative model for BO regeneration by means of charge state control of hydrogen," *Energy Procedia*, vol. 77, pp. 592–598, 2015, doi: 10.1016/j.egypro.2015.07.085.

[8] A. Ciesla née Wenham *et al.*, "Hydrogen-induced degradation," in *Proc. IEEE 7th World Conf. Photovolt. Energy Convers.*, 2018, pp. 0001–0008.

[9] T. Niewelt *et al.*, "Understanding the light-induced degradation at elevated temperatures: Similarities between multicrystalline and floatzone p-type silicon," *Prog. Photovolt.*, vol. 26, no. 8, pp. 533–542, 2017, doi: 10.1002/pip.2954.

[10] D. Chen *et al.*, "Hydrogen-induced degradation: Explaining the mechanism behind light- and elevated temperature-induced degradation in n- and p-type silicon," *Sol. Energy Mater. Sol. Cells*, vol. 207, 2020, Art. no. 110353, doi: 10.1016/j.solmat.2019.110353.

[11] J. Schmidt, D. Bredemeier, and D. C. Walter, "On the defect physics behind light and elevated temperature-induced degradation (LeTID) of multicrystalline silicon solar cells," *IEEE J. Photovolt.*, vol. 9, no. 6, pp. 1497–1503, Nov. 2019.

[12] F. Fertig *et al.*, "Mass production of p-type cz silicon solar cells approaching average stable conversion efficiencies of 22%," *Energy Procedia*, vol. 124, pp. 338–345, 2017, doi: 10.1016/j.egypro.2017.09.308.

[13] D. Chen *et al.*, "Evidence of an identical firing-activated carrier-induced defect in monocrystalline and multicrystalline silicon," *Sol. Energy Mater. Sol. Cells*, vol. 172, pp. 293–300, 2017, doi: 10.1016/j.solmat.2017.08.003.

[14] D. Chen *et al.*, "Hydrogen induced degradation: A possible mechanism for light- and elevated temperature-induced degradation in n-type silicon," *Sol. Energy Mater. Sol. Cells*, vol. 185, pp. 174–182, 2018, doi: 10.1016/j.solmat.2018.05.034.

[15] K. Ramspeck *et al.*, "Light induced degradation of rear passivated mc-Si solar cells," in *Proc. 27th Eur. Photovolt. Sol. Energy Conf. Exhib.*, 2012, pp. 861–865.

[16] M. Padmanabhan *et al.*, "Light-induced degradation and regeneration of multicrystalline silicon Al-BSF and PERC solar cells," *Phys. Status Solidi*, vol. 10, no. 12, pp. 874–881, 2016, doi: 10.1002/pssr.201600173.

[17] K. Petter *et al.*, "Dependence of LeTID on brick height for different wafer suppliers with several resistivities and dopants," in *Proc. 9th Int. Workshop Crystalline Silicon Sol. Cells*, 2016, pp. 1–17.

[18] C. E. Chan *et al.*, "Rapid stabilization of high-performance multicrystalline p-type silicon PERC cells," *IEEE J. Photovolt.*, vol. 6, no. 6, pp. 1473–1479, Nov. 2016.

[19] D. Bredemeier, D. Walter, S. Herlufsen, and J. Schmidt, "Lifetime degradation and regeneration in multicrystalline silicon under illumination at elevated temperature," *AIP Adv.*, vol. 6, no. 3, 2016, Art. no. 035119, doi: 10.1063/1.4944839.

[20] K. Nakayashiki *et al.*, "Engineering solutions and root-cause analysis for light-induced degradation in p-type multicrystalline silicon PERC modules," *IEEE J. Photovolt.*, vol. 6, no. 4, pp. 860–868, Jul. 2016.

[21] C. Sen *et al.*, "Annealing prior to contact firing: A potential new approach to suppress LeTID," *Sol. Energy Mater. Sol. Cells*, vol. 200, 2019, Art. no. 109938, doi: 10.1016/j.solmat.2019.109938.

[22] S. Liu *et al.*, "Impact of dark annealing on the kinetics of light- and elevated-temperature-induced degradation," *IEEE J. Photovolt.*, vol. 8, no. 6, pp. 1494–1502, Nov. 2018.

[23] D. Bredemeier, D. Walter, and J. Schmidt, "Light-induced lifetime degradation in high-performance multicrystalline silicon: Detailed kinetics of the defect activation," *Sol. Energy Mater. Sol. Cells*, vol. 173, pp. 2–5, 2017, doi: 10.1016/j.solmat.2017.08.007.

[24] F. Kersten, J. Heitmann, and J. W. Müller, "Influence of Al_2O_3 and SiN_x passivation layers on LeTID," *Energy Procedia*, vol. 92, pp. 828–832, 2016, doi: 10.1016/j.egypro.2016.07.079.

[25] C. Vargas *et al.*, "Carrier-induced degradation in multicrystalline silicon: Dependence on the silicon nitride passivation layer and hydrogen released during firing," *IEEE J. Photovolt.*, vol. 8, no. 2, pp. 413–420, Mar. 2018.

[26] U. Varshney *et al.*, "Evaluating the impact of SiN_x thickness on lifetime degradation in silicon," *IEEE J. Photovolt.*, vol. 9, no. 3, pp. 601–607, May 2019.

[27] U. Varshney *et al.*, "Controlling light- and elevated-temperature-induced degradation with thin film barrier layers," *IEEE J. Photovolt.*, vol. 10, no. 1, pp. 19–27, Jan. 2020.

[28] D. Bredemeier, D. C. Walter, R. Heller, and J. Schmidt, "Impact of hydrogen-rich silicon nitride material properties on light-induced lifetime degradation in multicrystalline silicon," *Phys. Status Solidi*, vol. 13, no. 8, 2019, Art. no. 1900201, doi: 10.1002/pssr.201900201.

[29] D. Bredemeier, D. C. Walter, R. Heller, and J. Schmidt, "Impact of silicon nitride film properties on hydrogen in-diffusion into crystalline silicon," in *Proc. 36th Eur. Photovolt. Sol. Energy Conf.*, 2019, pp. 112–115.

[30] D. C. Walter, D. Bredemeier, R. Falster, V. V. Voronkov, and J. Schmidt, "Easy-to-apply methodology to measure the hydrogen concentration in boron-doped crystalline silicon," *Sol. Energy Mater. Sol. Cells*, vol. 200, 2019, Art. no. 109970, doi: 10.1016/j.solmat.2019.109970.

[31] D. Lausch *et al.*, "Classification and investigation of recombination active defect structures in multicrystalline silicon solar-cells," in *Proc. 27th Eur. Photovolt. Sol. Energy Conf. Exhib.*, 2012, pp. 723–728, doi: 10.4229/27thEUPVSEC2012-2CO.13.4.

[32] W. A. Lanford and M. J. Rand, "The hydrogen content of plasma-deposited silicon nitride," *J. Appl. Phys.*, vol. 49, no. 4, 1978, Art. no. 2473, doi: 10.1063/1.325095.

[33] S. A. Schwarz, "Secondary ion mass spectroscopy," in *Encyclopedia of Materials: Science and Technology*. New York, NY, USA: Elsevier, 2001, pp. 8283–8290, doi: 10.1016/b0-08-043152-6/01482-0.

[34] A. E. T. Kuiper, "RBS and ERD analysis of semiconductor device materials," *Surf. Interface Anal.*, vol. 16, no. 1–12, pp. 29–35, 1990, doi: 10.1002/sia.740160110.

[35] S. Gerke, H.-W. Becker, D. Rogalla, R. Job, and B. Terheiden, "Model based prediction of the trap limited diffusion of hydrogen in post-hydrogenated amorphous silicon," *Phys. Status Solidi*, vol. 10, no. 11, pp. 828–832, 2016, doi: 10.1002/pssr.201600303.

[36] D. Abou-Ras, T. Kirchartz, and U. Rau, *Advanced Characterization Techniques for Thin Film Solar Cells*. Weinheim, Germany: Wiley, 2011.

[37] W. Beyer, "Hydrogen incorporation, stability, and release effects in thin film silicon," *Phys. Status Solidi*, vol. 213, no. 7, pp. 1661–1674, 2016, doi: 10.1002/pssa.201532976.

[38] W. Beyer and H. Mell, "Composition and thermal stability of glow-discharge a-Si:C:H and a-Si:N:H alloys," in *Disordered Semiconductors*. Berlin, Germany: Springer, 1987, pp. 641–658.

[39] D. Murley, I. French, S. Deane, and R. Gibson, "The effect of hydrogen dilution on the aminosilane plasma regime used to deposit nitrogen-rich amorphous silicon nitride," *J. Non-Crystalline Solids*, vol. 198–200, pp. 1058–1062, 1996, doi: 10.1016/0022-3093(96)00041-5.

[40] W. Beyer and H. F. W. Dekkers, "Microstructure characterization of amorphous silicon-nitride films by effusion measurements," *MRS Online Proc. Library*, vol. 910, 2005, Art. no. 605, doi: 10.1557/proc-0910-a06-05.

[41] S. Jafari *et al.*, "Composition limited hydrogen effusion rate of a-SiN_x:H passivation stack," in *AIP Conf. Proc.*, 2019, Art. no. 050004.

[42] D. N. R. Payne *et al.*, "Rapid passivation of carrier-induced defects in p-type multi-crystalline silicon," *Sol. Energy Mater. Sol. Cells*, vol. 158, pp. 102–106, 2016, doi: 10.1016/j.solmat.2016.05.022.

[43] S. W. Glunz, S. Rein, J. Y. Lee, and W. Warta, "Minority carrier lifetime degradation in boron-doped Czochralski silicon," *J. Appl. Phys.*, vol. 90, no. 5, pp. 2397–2404, 2001, doi: 10.1063/1.1389076.

[44] S. Jafari *et al.*, "Occurrence of sharp hydrogen effusion peaks of hydrogenated amorphous silicon film and its connection to void structures," *Phys. Status Solidi*, vol. 257, no. 9, 2020, Art. no. 2000097, doi: 10.1002/pssb.202000097.

[45] W. Beyer and H. Wagner, "Determination of the hydrogen diffusion coefficient in hydrogenated amorphous silicon from hydrogen effusion experiments," *J. Appl. Phys.*, vol. 53, no. 12, pp. 8745–8750, 1982, doi: 10.1063/1.330474.

[46] G. Dingemans, F. Einsele, W. Beyer, M. C. M. van de Sanden, and W. M. M. Kessels, "Influence of annealing and Al_2O_3 properties on the hydrogen-induced passivation of the Si/SiO_2 interface," *J. Appl. Phys.*, vol. 111, no. 9, 2012, Art. no. 093713, doi: 10.1063/1.4709729.

[47] A. van Wieringen and N. Warmoltz, "On the permeation of hydrogen and helium in single crystal silicon and germanium at elevated temperatures," *Physica*, vol. 22, no. 6–12, pp. 849–865, Jan. 1956, doi: 10.1016/S0031-8914(56)90039-8.

[48] M. Sheoran *et al.*, "Hydrogen diffusion in silicon from PECVD silicon nitride," in *Proc. 33rd IEEE Photovolt. Specialists Conf.*, 2008, pp. 1–4, doi: 10.1109/PVSC.2008.4922638.

[49] D. Bredemeier, D. C. Walter, and J. Schmidt, "Possible candidates for impurities in mc-Si wafers responsible for light-induced lifetime degradation and regeneration," *Sol. RRL*, vol. 2, no. 1, 2018, Art. no. 1700159, doi: 10.1002/solr.201700159.

[50] M. A. Jensen *et al.*, "Solubility and diffusivity: Important metrics in the search for the root cause of light- and elevated temperature-induced degradation," *IEEE J. Photovolt.*, vol. 8, no. 2, pp. 448–455, Mar. 2018.

[51] V. Verlaan, C. H. M. van der Werf, W. M. Arnoldbik, H. D. Goldbach, and R. E. I. Schropp, "Unambiguous determination of Fourier-transform infrared spectroscopy proportionality factors: The case of silicon nitride," *Phys. Rev. B*, vol. 73, no. 19, 2006, Art. no. 195333, doi: 10.1103/PhysRevB.73.195333.

[52] G. Dingemans *et al.*, "Stability of Al_2O_3 and Al_2O_3/a-SiNx:H stacks for surface passivation of crystalline silicon," *J. Appl. Phys.*, vol. 106, no. 11, Dec. 2009, Art. no. 114907, doi: 10.1063/1.3264572.